

# Inhibition of TGFBIp Expression by Lithium: Implications for *TGFBI*-Linked Corneal Dystrophy Therapy

Seung-Il Choi,<sup>1,2</sup> Bong-Yoon Kim,<sup>1,2</sup> Shorafidinkhuja Dadakhujaev,<sup>1,2</sup> James V. Jester,<sup>3</sup> Hyunmi Ryu,<sup>1,2</sup> Tae-im Kim,<sup>1,2</sup> and Eung Kweon Kim<sup>1,2,4,5</sup>

**PURPOSE.** The purpose of this study was to investigate the effects and molecular mechanisms of lithium on inhibition of TGFBIp expression as a potential therapy for *TGFBI*-linked corneal dystrophy.

**METHODS.** Primary culture corneal fibroblasts were isolated from the corneas of healthy subjects and patients with granular corneal dystrophy type 2 (GCD2) with a homozygous mutation in *TGFBI* R124H. Levels of TGFBIp and its mRNA in corneal fibroblasts treated with various lithium (LiCl) concentrations were analyzed by Western blot, RT-PCR, and quantitative real-time PCR.

**RESULTS.** LiCl treatment reduced the expression levels of normal and mutant TGFBIp in a dose- and a time-dependent manner. Furthermore, TGF- $\beta$ 1-induced TGFBIp expression decreased by 35% and 67% after treatment with 5 mM and 10 mM LiCl, respectively. LiCl decreased the level of pSmad3 (S423/425) in a dose-dependent manner. Furthermore, LiCl increased the level of pGSK-3 $\alpha/\beta$  (S21/9) in a dose-dependent manner. Also observed was the interaction between GSK-3 $\beta$  and Smad3, which was enhanced by lithium. In addition, Western blot analysis showed that the ratio of LC3-II/LC3-I in corneal fibroblasts increased after LiCl treatment. Cell viability at different doses was greater than 98%, indicating that LiCl did not induce significant corneal fibroblast death. Finally, the observed attenuating effects of LiCl on TGFBIp expression were not the results of cell death.

**CONCLUSIONS.** The accumulation of mutant TGFBIp ultimately leads to the histopathologic and clinical manifestations associated with *TGFBI*-linked corneal dystrophy. These data strongly suggest that lithium may be used for the prevention or treatment of this disease. (*Invest Ophthalmol Vis Sci.* 2011;52:3293–3300) DOI:10.1167/iovs.10-6405

From the <sup>1</sup>Corneal Dystrophy Research Institute, the <sup>2</sup>Department of Ophthalmology, and the <sup>4</sup>Severance Medical Research Institute, Yonsei University College of Medicine, Seoul, South Korea; the <sup>3</sup>Gavin Herbert Eye Institute, University of California Irvine, California; and the <sup>5</sup>Brain Korea 21 Project for Medical Science, Yonsei University, Seoul, South Korea.

Supported by the Converging Research Center Program through the National Research Foundation of Korea (NRF) funded by the Ministry of Education, Science, and Technology (Grant 2009-0082186) and by the Mid-Career Researcher Program through an NRF grant funded by the Ministry of Education, Science, and Technology (Grant 2010-0000324).

Submitted for publication August 13, 2010; revised December 14, 2010; accepted January 3, 2011.

Disclosure: S.-I. Choi, None; B.-Y. Kim, None; S. Dadakhujaev, None; J.V. Jester, None; H. Ryu, None; T. Kim, None; E.K. Kim, None

Corresponding author: Eung Kweon Kim, Department of Ophthalmology, Yonsei University College of Medicine, 250 Seongsanno, Seodaemun-gu, Seoul 120-752, Korea; eungkkim@yuhs.ac.

Transforming growth factor- $\beta$ -induced gene protein (TGFBIp), also known as  $\beta$ ig-h3 protein, is secreted in response to transforming growth factor- $\beta$  (TGF- $\beta$ ) in human adenocarcinoma cells and other cell types.<sup>1</sup> In addition, this protein exhibits tumor suppressive activity.<sup>2,3</sup> More recently, reports have shown that TGFBIp deficiency in mice induces cell proliferation and spontaneous tumor development.<sup>4</sup> The *TGFBI* gene encodes a highly conserved 683-amino acid protein that contains a secretory signal sequence and an Arg-Gly-Asp motif that serves as a ligand recognition site for integrins.<sup>1</sup> TGFBIp is a component of the extracellular matrix, where it mediates cell adhesion and migration by interacting with integrins.<sup>5–7</sup>

Granular corneal dystrophy type 2 (GCD2, also called Avelino corneal dystrophy) is an autosomal dominant disorder caused by a point mutation (R124H) in the *TGFBI* gene on chromosome 5q31.<sup>1</sup> Age-dependent progressive accumulation of hyaline and amyloid in the corneal stroma is a hallmark of GCD2, which is characterized by TGFBIp production in the corneal epithelia and stroma, thereby interfering with corneal transparency.<sup>1,8,9</sup> To date, 38 mutations in the *TGFBI* gene have been implicated in corneal dystrophies. Interestingly, different mutations cause unique corneal dystrophy phenotypes. Thus, though R124H is associated with GCD2, R124C is associated with lattice corneal dystrophy type 1, R555W is associated with granular corneal dystrophy type 1, and R555Q is associated with Thiel-Behnke corneal dystrophy.<sup>10</sup>

Glycogen synthase kinase-3 (GSK-3) is an intracellular enzyme involved in several cellular events.<sup>11</sup> In particular, GSK-3 is well established as a component of the Wnt signaling pathway. Binding of Wnts to their receptors results in GSK-3 inhibition and a subsequent increase in  $\beta$ -catenin levels.<sup>12,13</sup> In addition, GSK-3 is regulated by other signaling pathways, including those involving AKT, and also serves as an upstream regulator of other transcription factors and cellular proteins.<sup>11,14,15</sup>

GSK-3 inactivation generally results in antiapoptosis. A number of studies have demonstrated that lithium inhibits GSK-3,<sup>16–21</sup> and direct inhibition of GSK-3 activity by lithium has been proved.<sup>18,19</sup> GSK-3 is generally considered to play a proapoptotic role, and its inhibition results in cytoprotection.<sup>22</sup> Lithium also indirectly inhibits GSK-3 by triggering the phosphorylation of GSK-3 at Ser21/Ser9.<sup>23–25</sup> Increasing evidence suggests that lithium elicits its neuroprotective effects primarily by inhibiting GSK-3.<sup>26</sup> Besides direct inhibition, lithium can inhibit GSK-3 indirectly through the phosphorylation of GSK-3 $\alpha$  at Ser21 and GSK-3 $\beta$  at Ser9 by multiple mechanisms, including the activation of PKA,<sup>27</sup> phosphatidylinositol 3-kinase (PI3-K)-dependent AKT,<sup>23</sup> protein kinase C (PKC),<sup>28</sup> and GSK-3 autoregulation.<sup>25,29</sup>

Recent reports demonstrated that the transcription factor Smad3/4 is a novel GSK-3 target in neurons.<sup>30</sup> Smad3/4 is a downstream mediator of TGF- $\beta$ -mediated signaling pathways.<sup>31</sup> Binding of TGF- $\beta$  to its serine/threonine kinase recep-

tor leads to Smad2 and Smad3 phosphorylation. Phosphorylated Smad (pSmad) proteins then form a complex with Smad4 followed by translocation to the nucleus, where they interact with other gene-specific transcription factors to regulate gene expression.<sup>31,32</sup> Smad3/4 plays a prominent role in regulating the expression of proteins involved in neuronal survival/death, differentiation, and plasticity.<sup>33,34</sup> Studies have demonstrated that TGF- $\beta$  can induce the phosphorylation of Smad3 at Thr179, Ser204, and Ser208. Furthermore, GSK-3 phosphorylates Smad3 directly at Ser204.

These data suggest that the inhibition of mutant TGFBIp (mut-TGFBIp) production through the regulation of TGF- $\beta$  signaling with GSK-3 inhibitors may be a potential therapy for TGFBI-linked corneal dystrophy. Therefore, we investigated the effects of lithium treatment on TGFBIp expression. We found that these treatments reduced TGFBIp expression dramatically in corneal fibroblasts. To our knowledge, this is the first demonstration of decreased TGFBIp expression mediated through the inhibition of TGF- $\beta$  signaling by lithium. These results suggest that the use of clinical trials of lithium to treat TGFBI-linked corneal dystrophy is a rational strategy.

## MATERIALS AND METHODS

### Materials

LiCl and KCl were obtained from Sigma-Aldrich (St. Louis, MO). Recombinant TGF- $\beta$ 1 was obtained from R&D Systems (Minneapolis, MN). Enhanced chemiluminescence substrate (SuperSignal West Pico Chemiluminescent Substrate, Pierce) was purchased from Pierce (Rockford, IL).

### Isolation and Culture of Primary Corneal Fibroblasts

Normal and homozygote primary corneal fibroblasts were prepared using previously described methods.<sup>35</sup> Donor confidentiality was maintained in accordance with the Declaration of Helsinki, and the conduct of the study was approved by the Severance Hospital IRB Committee (CR04124), Yonsei University. GCD2 was diagnosed by DNA sequence analysis for TGFBI gene mutations. After removal of the corneal button for keratoplasty, the remaining corneal rims were harvested for normal corneal fibroblast culture. Medical records of donors from the eye bank of Yonsei University Severance Hospital did not show any genetic or systemic metabolic disease. Fibroblasts grown from pieces of corneal rims were treated as healthy controls, and DNA sequencing analysis was performed to verify genetic normality of the *BIGH3* gene. The healthy human corneal fibroblast cells<sup>36</sup> were cultured in DMEM supplemented with 10% fetal bovine serum at 37°C in a humidified incubator with 95% air and 5% CO<sub>2</sub>.

### Cell Treatment with Lithium

Lithium was freshly dissolved in phosphate-buffered saline (PBS; Gibco-BRL, Carlsbad, CA) at room temperature before use. To examine

the effects of lithium on TGFBIp protein expression, corneal fibroblasts were incubated with 10 to 100 mM LiCl and then analyzed by immunoblot analysis.

### RNA Isolation and RT-PCR

For the amplification of TGFBI and  $\beta$ -actin, total RNA was isolated from corneal fibroblasts by extraction in reagent (Trizol; Invitrogen Life Technologies, Carlsbad, CA). cDNA synthesis and DNA amplification were performed (Superscript One-Step RT-PCR System; Invitrogen Life Technologies) and primers (Table 1). Amplification products were visualized by electrophoresis in 1.2% agarose gels containing ethidium bromide.

### Real-Time PCR

Primers for the human TGFBI and  $\beta$ -actin specific genes were designed according to the published sequences available in GenBank using Primer3, as shown in Table 1. For the analysis of each sample, gene expression levels were calibrated using  $\beta$ -actin expression levels as an internal control. Two micrograms of total RNA was reverse-transcribed into cDNA using reverse transcriptase (Superscript II; Invitrogen) and an Oligo (dT) primer (Invitrogen). The cDNA reaction was amplified in triplicate by real-time PCR (Exicycler; Bioneer, Deajeon, South Korea) in a final volume of 50  $\mu$ L using SYBR Green master mix reagent (AccurPower GreenStar qPCR PreMix; Bioneer) and appropriate software (Exicycler version 3.1; Bioneer).  $\beta$ -Actin, a constitutively expressed housekeeping gene, was amplified under the same conditions and used to normalize reactions. To ensure the specificity of the reaction, the size of the PCR product for each gene was verified by 1.3% agarose gel electrophoresis. Results were evaluated by data analysis with spreadsheet software (Excel; Microsoft, Redmond, WA). All PCRs were performed under the following conditions: 2 minutes at 50°C, 5 minutes at 95°C, and 40 cycles of 15 seconds at 95°C and 45 seconds at 58°C in 96-well optical reaction plates (Bioneer). The specificity of amplicons was verified by melting curve analysis (60°C–95°C) after 40 cycles and agarose gel electrophoresis. Two replicates for each sample were used for real-time PCR analysis, and three technical replicates were analyzed for each replicate. Results of quantitative RT-PCR were assessed by *t*-test.

### Preparation of Cell Lysates, Immunoprecipitation, and Immunoblot Analysis

Cell lysates from corneal fibroblasts were prepared in radioimmunoprecipitation assay buffer (RIPA buffer; 150 mM/L NaCl, 1% NP-40, 0.5% deoxycholate, 0.1% SDS, 50 mM/L Tris-HCl, pH 7.4) containing protease inhibitors (Complete Mini Protease Inhibitor Cocktail Tablet, catalog no. 1836170; Roche, Indianapolis, IN) and phosphatase inhibitors (PhosSTOP, catalog no. 04906845001; Roche). Crude cell lysates were centrifuged at 10,000g for 10 minutes at 4°C to remove nuclear fragments and tissue debris. A portion of the supernatant was used to determine the total protein concentration using a bicinchoninic acid kit (Pierce).

Total cell lysate (5 mg protein) was subjected to immunoprecipitation with anti-GSK-3 and anti-Smad3 antibodies, as indicated, overnight at 4°C with gentle agitation, followed by incubation (Protein A/G

TABLE 1. Primer Sequences Used for RT-PCR and Real-Time PCR Analysis

Gene	Sequence	Accession No.	Amplicon Length (bp)	Analysis Method
TGFBI	F: 5'-AGCAGCCCTACCACTCTCAA-3' R: 5'-GACATTGCTGACCAGGGAGT-3'	NM_000358	196	RT-PCR
$\beta$ -Actin	F: 5'-GGACTTCGAGCAAGAGATGG-3' R: 5'-AGCACTGTGTGGCGTACAG-3'	NM_001101	234	
TGFBI	F: 5'-GTCCACAGCCATTGACCTTT-3' R: 5'-ACCGCTCACTCCAGAGAGA-3'	NM_000358	82	Real-time PCR
$\beta$ -Actin	F: 5'-GGCATCCTCACCTGAAGTA-3' R: 5'-AGGTGTGGTGCAGATTTTC-3'	NM_001101	65	

F, forward primer; R, reverse primer.

Plus-Agarose; Invitrogen) for 2 to 4 hours at 4°C. After binding, the beads were washed extensively three times with RIPA buffer and then mixed with 2× SDS sample buffer and boiled for 5 minutes.

For immunoblot analysis, total cellular protein was subjected to electrophoresis on 10% Tris-glycine SDS polyacrylamide gels. Proteins were transferred onto polyvinylidene difluoride membranes (Millipore Corp., Bedford, MA), blocked in 5% dry milk in Tris-buffered saline containing Tween-20 (TBS-T) (0.02 M Tris/0.15 M NaCl, pH 7.5, 0.1% Tween 20) at room temperature for 1 hour, washed three times with TBS-T, and incubated with antibodies against TGFBIp (0.2 μg/mL; catalog no. AF2935; R&D Systems), β-actin (1:5000 dilution; catalog no. A-5441; Sigma-Aldrich), and GSK-3α/β, pGSK-3α/β, Smad3, and pSmad3 (1:1000 dilution; Cell Signaling Technology, Beverly, MA) overnight at 4°C. After three washes with TBS-T, blots were incubated with HRP-conjugated secondary antibody (anti-mouse IgG [1:5000 dilution; catalog no. NA931V] or anti-rabbit IgG [1:5000 dilution; catalog no. NA934V]; Amersham Pharmacia Biotechnology, Piscataway, NJ) at room temperature for 1 hour. Western blot analysis was visualized using enhanced chemiluminescence (Pierce). Immunoreactive protein bands were scanned at two intensities, and the optical densities of the bands were quantified computationally with the use of ImageJ software (developed by Wayne Rasband, National Institutes of Health, Bethesda, MD; available at <http://rsb.info.nih.gov/ij/index.html>). The background was corrected through subtraction, and protein levels were normalized relative to the intensity of the corresponding β-actin protein bands.

**Cell Viability**

Corneal fibroblasts were plated in 96-well plates at a density of 10,000 cells/well and incubated overnight. Cell proliferation was determined

(CellTiter 96 Aqueous One Solution Reagent Cell Proliferation Assay Kit; Promega, Madison, WI) and tetrazolium (3-[4,5-dimethylthiazol-2-yl]-5-(3-carboxymethoxyphenyl)-2-[4-sulfophenyl]-2H-tetrazolium, inner salt; MTS) (catalog no. G3580; Promega). Briefly, the culture medium was removed, and 20 μL MTS solution was added to each well containing 100 μL culture medium. Cultures were incubated at 37°C for 2 to 4 hours under 95% humidity and 5% CO<sub>2</sub>. Optical density was measured at 450 nm using a plate reader.

**Statistical Analysis**

The results were evaluated statistically for significance (*P* < 0.05) using one-way analysis of variance followed by the Newman-Keuls multiple comparison test. Data are expressed as mean ± SD. All data were processed using scientific graphing analysis software (Prism, version 4.0; GraphPad Software Inc., San Diego, CA).

**RESULTS**

**TGFBIp Expression Is Downregulated by Lithium in Corneal Fibroblasts**

Recently, several studies have revealed that inhibitors of GSK-3 can downregulate TGFBIp expression by blocking TGF-β signaling.<sup>30-32</sup> To test this hypothesis, we analyzed levels of TGFBIp in primary corneal fibroblasts treated with lithium, a known GSK-3 inhibitor. Western blot analysis showed that lithium reduced levels of TGFBIp in a dose- (Fig. 1A) and a time-dependent manner (Fig. 1B). We next examined the ef-

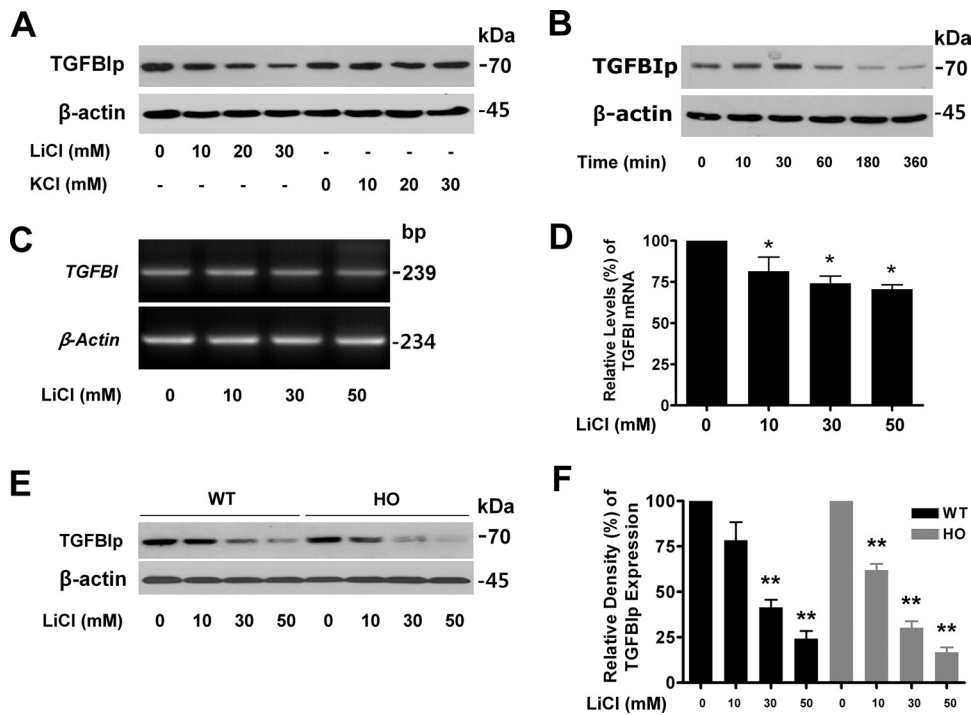


**FIGURE 1.** LiCl reduces TGFBIp expression in primary cultured corneal fibroblasts. (A) A healthy corneal fibroblast cell line was treated with the indicated amounts of LiCl or KCl for 12 hours. KCl was used as a control. The levels of TGFBIp were assessed by Western blot analysis. (B) A healthy corneal fibroblast cell line was treated with 10 mM LiCl for the indicated times. The levels of TGFBIp were assessed by Western blot analysis. (C) The level of TGFBI mRNA in healthy corneal fibroblast cells treated with the indicated concentrations of LiCl for 12 hours was measured by RT-PCR. (D) Quantification of the data presented in (C). (E) WT and HO primary corneal fibroblasts were treated with the indicated amounts of LiCl for 12 hours. The levels of TGFBIp were assessed by Western blot analysis. β-Actin served as a loading control. (F) Quantification of the data presented in (E). All signals were quantified using NIH Image J. Values represent the mean ± SD of at least three independent experiments. Statistical analysis was performed using one-way analysis of variance followed by the Newman-Keuls multiple comparison test. \**P* < 0.05; \*\**P* < 0.01 with LiCl versus without LiCl.



fects of lithium on *TGFBI* mRNA expression. Quantitative RT-PCR showed that treatment with LiCl for 12 hours resulted in decreased *TGFBI* mRNA expression in a dose-dependent manner (Fig. 1C). Quantitative analysis revealed that treatments with 10 mM, 30 mM and 50 mM LiCl significantly decreased *TGFBI* mRNA expression by approximately  $81.43\% \pm 8.73\%$ ,  $74.10\% \pm 4.41\%$ , and  $70.60\% \pm 2.69\%$ , respectively, relative to  $\beta$ -actin, which was used as a control ( $P < 0.05$ ) (Fig. 1D). Taken together, these results suggest that TGFBIp regulation occurs at the level of transcription.

In addition, we analyzed the expression of mut-TGFBIp in GCD2 homozygous (HO) corneal fibroblasts after lithium treatment to test whether the inhibitor also blocked the expression of GCD2-linked mutant TGFBIp. Treatment of wild-type (WT) corneal fibroblasts with 10, 30, and 50 mM LiCl for 12 hours reduced TGFBIp levels by  $78.37\% \pm 10.00\%$ ,  $41.43\% \pm 4.25\%$ , and  $24.33\% \pm 4.14\%$ , respectively, compared with untreated fibroblasts ( $P < 0.01$ ) (Figs. 1E, 1F). Further, LiCl treatment at the same concentrations decreased TGFBIp expression by approximately  $61.96\% \pm 3.51\%$ ,  $30.21\% \pm 3.63\%$ , and  $16.75\% \pm 2.74\%$ , respectively, in GCD2 HO corneal fibroblasts ( $P < 0.01$ ) (Figs. 1E, 1F).

### Induction of TGFBIp Expression by TGF- $\beta$ 1 Is Inhibited by Lithium Treatment

TGFBIp was first identified in an adenocarcinoma cell line, where it was found to be upregulated on TGF- $\beta$  treatment. Therefore, we examined whether TGFBIp expression could also be induced by TGF- $\beta$  treatment in a corneal fibroblast cell line. Our data demonstrate that TGF- $\beta$ 1 induced the expression of TGFBIp in a dose- (Fig. 1A) and a time-dependent manner (Fig. 1B). Next, to investigate the effect of lithium on the induction of TGFBIp expression, corneal fibroblasts pretreated with TGF- $\beta$ 1 for 2 hours were subsequently treated with 10, 30, and 50 mM LiCl for 12 hours. As shown Figures 2C and 2D, 10, 30, and 50 mM lithium inhibited TGF- $\beta$ -induced TGFBIp levels by  $58.11\% \pm 9.06\%$ ,  $32.46\% \pm 5.79\%$ , and  $14.80\% \pm$

$3.94\%$ , respectively, compared with samples treated only with TGF- $\beta$ 1.

### Lithium Inhibits TGF- $\beta$ Signaling by Inhibition of Smad3 Phosphorylation

At least two mechanisms are conceivable for how LiCl decreases TGFBIp protein levels: LiCl enhances TGFBIp degradation or decreases TGFBIp biosynthesis. After identification of Smad3/GSK-3 complexes, Guo et al.<sup>37</sup> suggested that GSK-3 can activate Smad3. Further, lithium is well established as a GSK-3 inhibitor. Therefore, we examined the effects of LiCl on TGFBIp expression by investigating the TGF- $\beta$  signaling pathway. Treatment of corneal fibroblasts with 10, 30, and 50 mM LiCl reduced Smad3 phosphorylation (S423/425) by  $46.09\% \pm 5.53\%$ ,  $31.29\% \pm 6.70\%$ , and  $20.37\% \pm 6.29\%$ , respectively (Figs. 3A, 3B). In addition, LiCl interacts with GSK-3 $\alpha/\beta$  and negatively regulates its activity (Fig. 3A, 3C, 3D). Treatment of corneal fibroblasts with 10, 30, and 50 mM LiCl for 12 hours increased GSK-3 $\alpha$  phosphorylation significantly by  $317.3\% \pm 38.00\%$ ,  $401.0\% \pm 43.86\%$ , and  $512.0\% \pm 23.90\%$ , respectively ( $P < 0.01$ ; Fig. 3A, 3C). GSK-3 $\beta$  phosphorylation also increased significantly (Figs. 3A, 3D). Taken together, these results suggest that the observed lithium-induced decrease in TGFBIp levels was caused by the inhibition of TGF- $\beta$  signaling.

### Interaction of Smad3 with GSK-3 $\beta$

To examine whether Smad3 interacts with GSK-3 $\beta$  in corneal fibroblasts, we used healthy corneal fibroblasts. Endogenous GSK-3 $\beta$  was detected by the anti-GSK-3 $\beta$  antibody. When the lysates were immunoprecipitated with the anti-GSK-3 $\beta$  antibody, Smad3 was detected in the GSK-3 immune complex (Fig. 4A, lane 3). To examine the effect of LiCl on the interaction between GSK-3 $\beta$  and Smad3, we used lysates of corneal fibroblasts treated with 0, 30, and 50 mM LiCl concentration. When the lysates were immunoprecipitated with the anti-Smad3 antibody, detection of GSK-3 $\beta$  increased in the GSK-3

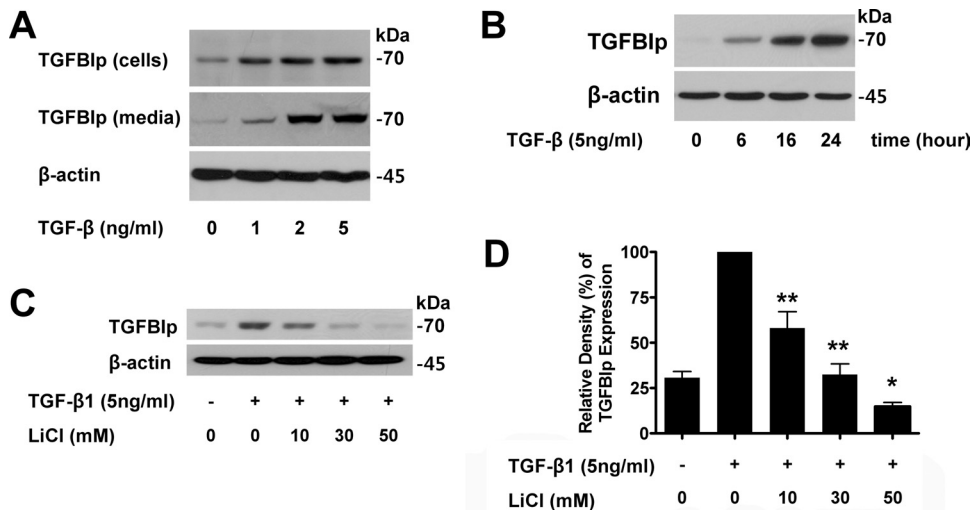
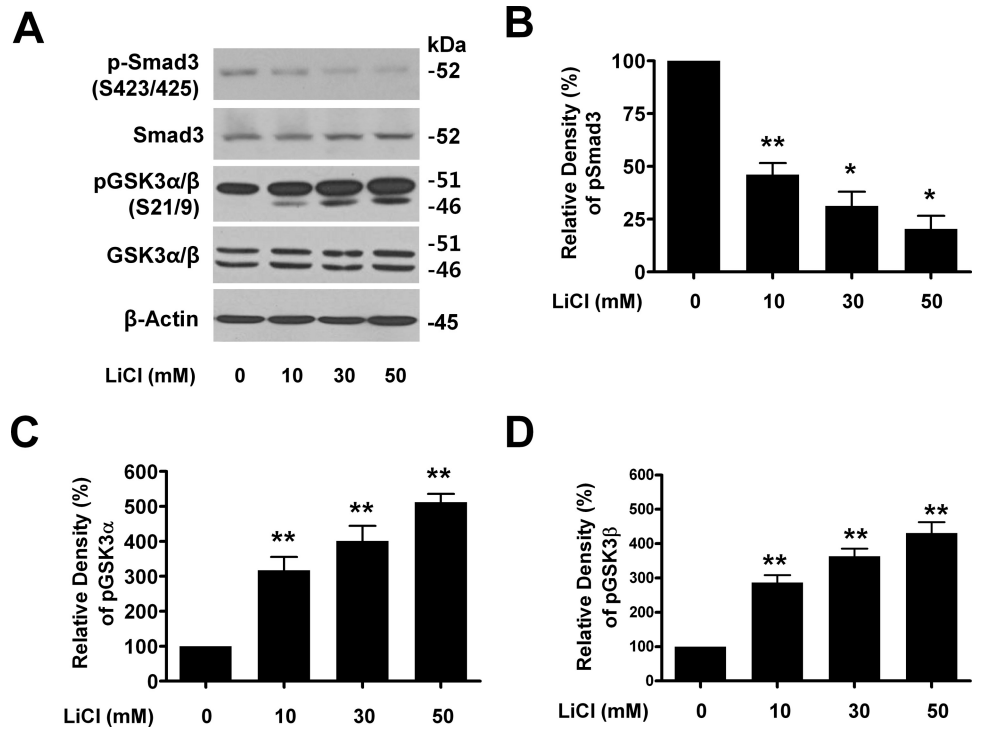


**FIGURE 2.** TGF- $\beta$ 1-induced TGFBIp expression is inhibited by LiCl. (A) A healthy corneal fibroblast cell line was treated with the indicated amounts of TGF- $\beta$ 1 for 12 hours. Cell lysates and media were analyzed for TGFBIp by Western blot analysis. (B) A healthy corneal fibroblast cell line was treated with 5 ng/mL TGF- $\beta$ 1 for the indicated times. TGFBIp levels were analyzed by Western blot. (C) Healthy corneal fibroblasts pretreated with 5 ng/mL TGF- $\beta$ 1 for 2 hours were cultured with 10 to 50 mM LiCl for 12 hours. TGFBIp levels were analyzed by Western blot. (D) Quantification of data presented in (C). The levels of TGFBIp were quantified using NIH Image J software and normalized to  $\beta$ -actin. Values represent the mean  $\pm$  SD of three independent experiments. Statistical analysis was performed using one-way analysis of variance followed by the Newman-Keuls multiple comparison test. \* $P < 0.05$ ; \*\* $P < 0.01$  with LiCl versus without LiCl.

**FIGURE 3.** LiCl inhibits TGF- $\beta$  signaling by promoting Smad3 dephosphorylation. **(A)** Healthy corneal fibroblast cells were treated with the indicated amounts of LiCl for 12 hours. Levels of pSmad3 (S423/425), Smad3, pGSK-3 $\alpha/\beta$ , p- $\beta$ -catenin, and  $\beta$ -catenin were assessed by Western blot. **(B)** Quantification of pSmad3 (S423/425) levels using NIH Image J software and normalized to total Smad3. **(C)** Healthy corneal fibroblast cells were treated with the indicated amounts of LiCl for 12 hours. Levels of pGSK-3 $\alpha$  were assessed by Western blot, quantified using NIH Image J software, and normalized to total GSK-3 $\alpha$ . **(D)** Healthy corneal fibroblasts were treated with the indicated amounts of LiCl for 12 hours. Levels of pGSK-3 $\beta$  were quantified using NIH Image J software and normalized to total GSK-3 $\alpha/\beta$ . Values represent the mean  $\pm$  SD of three independent experiments. Statistical analysis was performed using one-way analysis of variance followed by the Newman-Keuls multiple comparison test. \* $P < 0.05$ ; \*\* $P < 0.01$  with LiCl versus without LiCl.



immune complex obtained by LiCl treatment compared with the GSK-3 immune complex from no LiCl treatments (Fig. 4B, lane 3). In our hands, interactions between Smad3 and GSK-3 $\beta$  were not different during treatment with 30 and 50 mM LiCl. Together, these results suggest that lithium may regulate the intracellular TGF- $\beta$  signaling by the interactions of GSK-3 and Smad3 proteins.

**Lithium Induces Autophagy**

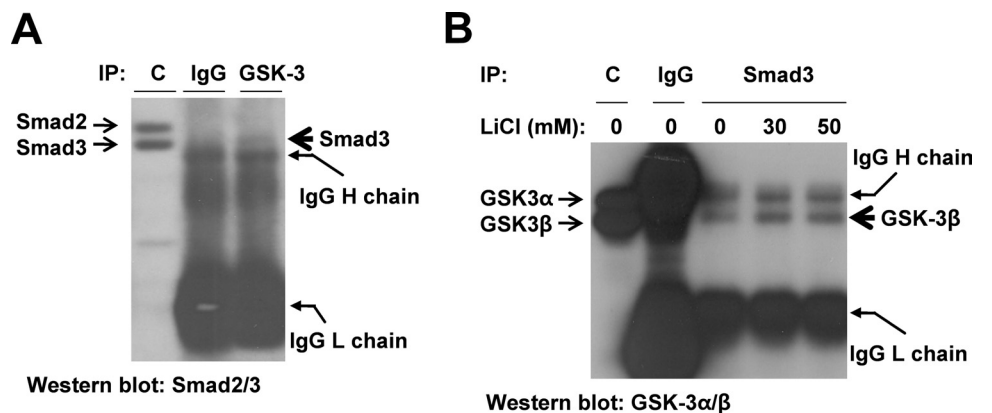
Reports have shown that lithium induces autophagy by way of the PI3K signaling pathway.<sup>38</sup> Previously, we demonstrated that the activation of autophagy enhances the cytosolic clearance of accumulated mut-TGFBIp in primary cultured GCD2 corneal fibroblasts (Choi et al., manuscript submitted). Thus, we investigated whether lithium activates autophagy in corneal fibroblasts. During autophagy, a cytosolic form of the microtubule-associated protein light chain 3-I (LC3-I) is conjugated to phosphatidylethanolamine to form LC3 phosphatidyle-

thanolamine conjugate (LC3-II), which is recruited to autophagosomal membranes. Both the ratio of LC3-II to LC3-I and the amount of LC3-II can be used to monitor autophagosome formation.<sup>39,40</sup> Therefore, it was used to monitor autophagy in this study. After treatment with 10, 30, and 50 mM LiCl for 12 hours in corneal fibroblasts, the ratio of LC3-II/LC3-I increased by 1.09  $\pm$  0.1-, 1.60  $\pm$  0.19-, and 2.56  $\pm$  0.24-fold, respectively ( $P < 0.01$ ), over the control (Figs. 5A, 5B). These results suggest that lithium not only inhibits TGFBIp expression, it also enhances the cytosolic clearance of accumulated mut-TGFBIp in corneal fibroblasts.

**Lithium Is Not Toxic to Primary Cultured Corneal Fibroblasts**

To assess the cytotoxicity of LiCl, primary corneal fibroblasts were incubated with LiCl, and cell viability was measured by the MTT assay. As shown in Figure 6, cell viability was greater

**FIGURE 4.** Physical interaction between GSK-3 and Smad3 in healthy corneal fibroblasts treated with LiCl. **(A)** The interaction between GSK-3 and Smad3 was determined by coimmunoprecipitation (co-IP) of GSK-3 using an anti-GSK-3 $\alpha/\beta$  antibody followed by Western blot with anti-Smad3 antibody. **(B)** Direct interaction between Smad3 and GSK-3 $\beta$  was determined by co-IP of Smad3 using an anti-pSmad3 antibody followed by Western blot with anti-GSK-3 $\alpha/\beta$  antibody. C, increased interaction between pSmad3 and pGSK-3 $\beta$  by LiCl. The interaction between GSK-3 and Smad3 was highly enhanced in corneal fibroblasts treated with the indicated LiCl concentration. Direct interaction between Smad3 and GSK-3 $\beta$  was determined by co-IP of Smad3 using an anti-pSmad3 antibody followed by Western blot with anti-GSK-3 $\alpha/\beta$  antibody. As a control, normal IgG alone was directly immunoprecipitated with anti-GSK-3 and anti-Smad3 (lanes 4 and 5), respectively. As a control, normal IgG alone was directly immunoprecipitated with anti-GSK-3 and anti-Smad3.



As a control, normal IgG alone was directly immunoprecipitated with anti-GSK-3 and anti-Smad3 (lanes 4 and 5), respectively. As a control, normal IgG alone was directly immunoprecipitated with anti-GSK-3 and anti-Smad3.

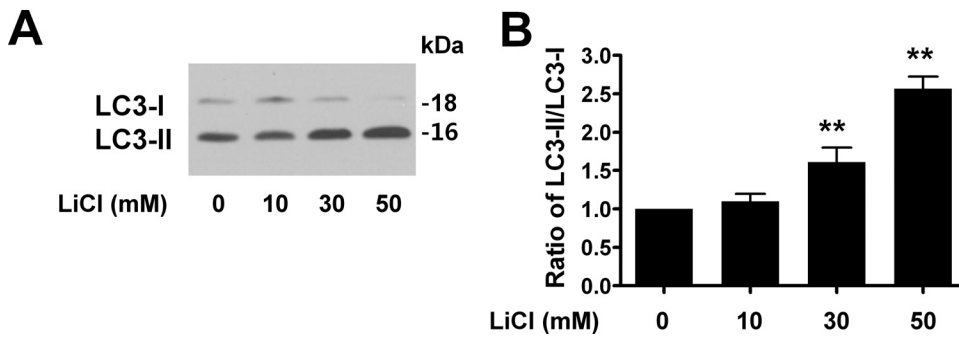


**FIGURE 5.** Lithium induces autophagy in corneal fibroblasts. (A) A healthy corneal fibroblast cell line was treated with the indicated amounts of LiCl for 12 hours. Protein levels of LC3 were assessed by Western blot. (B) LC3-II levels were quantified using NIH Image J software and normalized to LC3-I. Values represent the mean  $\pm$  SD of three independent experiments. Statistical analysis was performed using one-way analysis of variance followed by the Newman-Keuls multiple comparison test. \*\* $P < 0.01$  with LiCl versus without LiCl.

than 98% after treatment with four different doses of LiCl, indicating that LiCl did not result in significant cell death with the concentrations tested. Taken together, the observed attenuating effects of LiCl on TGFBIp expression were not due to corneal fibroblast cell death.

## DISCUSSION

There is no prevention or cure for *TGFBI*-linked corneal dystrophy. Thus, there is great hope for the development of novel therapies. To our knowledge, this is the first study describing the impact of lithium on specimens from *TGFBI*-linked corneal dystrophy patients. Here, we show an effective decrease in TGFBIp expression with lithium without cytotoxic effects. Furthermore, we confirmed lithium's role in the stimulation of autophagy in corneal fibroblasts. These findings strongly suggest that lithium may be used for the prevention or treatment for *TGFBI*-linked corneal dystrophies.

TGFBI is a secreted protein induced by TGF- $\beta$  in human adenocarcinoma cells and other human cell types.<sup>1</sup> This protein exhibits tumor suppressive function.<sup>2,3</sup> We have also shown that TGFBIp expression can be induced by TGF- $\beta$  in a dose-dependent manner and that lithium inhibits this induction in corneal fibroblasts. Thus, these results suggest that lithium may also have a potential role in inhibiting the TGF- $\beta$  signaling pathway.

Lithium was discovered in 1996 by Klein and Melton as a reversible GSK-3 inhibitor.<sup>19</sup> Studies have established that lithium reduces GSK-3 activity in two ways.<sup>41</sup> As a direct inhibitor, lithium competes with magnesium ions for GSK-3 binding.<sup>42</sup> Alternatively, as an indirect inhibitor, lithium increases the inhibitory N-terminal serine phosphorylation of GSK-3, which inactivates enzyme function. More recently, Millet et al.<sup>43</sup> have suggested that GSK-3 activity negatively regulates the TGF- $\beta$  signaling pathway.<sup>43</sup> These results suggest that lithium can affect genes regulated by TGF- $\beta$  signaling. Based on these results, we hypothesized that a GSK-3 inhibitor can be used as a potential therapeutic agent for *TGFBI*-linked corneal dystrophies. Therefore, we examined the role of lithium on the

expression of TGFBIp in WT and GCD2 corneal fibroblasts. Here, we have shown that lithium may prevent or treat *TGFBI*-linked corneal dystrophies by inhibiting TGF- $\beta$  signaling.

The TGF- $\beta$  signaling pathway has been implicated as a regulator in numerous cellular and physiological processes, including extracellular matrix homeostasis.<sup>16</sup> This pathway is initiated by the binding of TGF- $\beta$  to type I (T $\beta$ RI) and type II TGF- $\beta$  receptors (T $\beta$ RII), both of which are serine/threonine kinases. The activated receptor complex phosphorylates the downstream transcription factors Smad2 and Smad3, leading to their association with Smad4. The Smad complex then becomes concentrated in the nucleus and regulates the expression of target genes.<sup>32</sup> These steps are tightly controlled to ensure that Smad2/3 transmits signals from the plasma membrane to the nucleus. Therefore, the decrease in TGFBIp expression induced by lithium treatment is consistent with the observed reduction in Smad3 phosphorylation in the presence of the inhibitor (Fig. 3A).

However, although controlling Smad activity is crucial for proper TGF- $\beta$  signaling and its related factors, the specific mechanism(s) involved in the lithium-induced decrease in Smad3 phosphorylation remains unknown. More recently, Guo et al.<sup>37</sup> have shown that nonactivated Smad3, but not Smad2, undergoes proteasome-dependent degradation caused by the concerted action of the scaffolding protein Axin and its associated kinase, GSK-3 $\beta$ . Smad3 interacts physically with Axin and GSK-3 $\beta$  only in the absence of TGF- $\beta$ . Reduction in the expression or activity of Axin/GSK-3 $\beta$  leads to increased Smad3 stability and transcriptional activity without affecting TGF- $\beta$  receptors or Smad2. In contrast, overexpression of these proteins promotes Smad3 basal degradation and desensitizes cells to TGF- $\beta$ .<sup>37</sup> However, in this study, the mechanism of TGFBIp reduction in response to lithium may be mediated by the inhibition of TGF- $\beta$  signaling through decreased Smad3 phosphorylation without a reduction in total Smad3 protein. In addition, Millet et al.<sup>43</sup> demonstrated that TGF- $\beta$  induces phosphorylation at three sites within the Smad3 linker region in addition to two C-terminal residues. GSK-3 is responsible for phosphorylating one of these sites, namely Ser204. Although

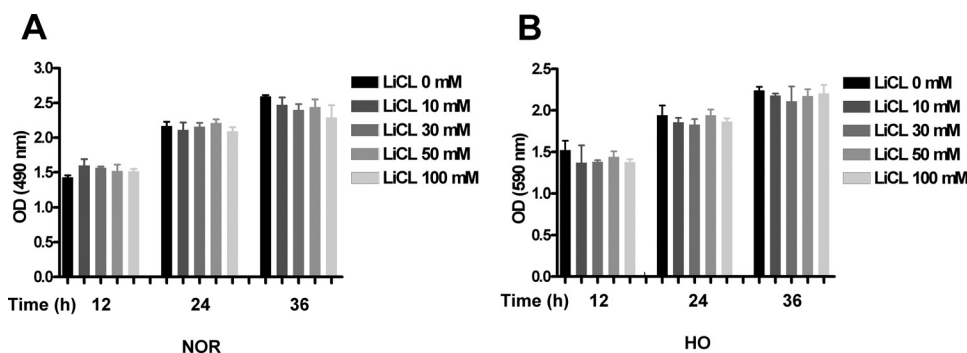


**FIGURE 6.** LiCl is not toxic to corneal fibroblasts. WT (A) and HO (B) corneal fibroblasts were treated with different concentrations of LiCl (0–100 mM) for the indicated times (12–36 hours). Cell viability was analyzed by the MTT assay. Cell viability was calculated using the following: MTS optical density (OD) value of sample/MTS OD value of control (cells treated with PBS).



we did not assay Smad3 (Ser204) phosphorylation, our results showed decreased Smad3 phosphorylation at S423/425 and increased interaction between Smad3 and GSK-3 $\beta$  in lithium-treated cells. Thus, our findings reveal a novel aspect of Smad3 signaling that controls the final amplitude of TGF $\beta$  expression and the cellular responses to TGF- $\beta$ .

The proteasome and autophagy/lysosomal pathways are the major routes for the clearance of cytosolic protein. Although the narrow proteasome barrel precludes entry of oligomers/aggregates of aggregate-prone intracellular proteins, such substrates can be degraded by autophagy. We have previously shown that TGF $\beta$ IP is degraded by the lysosome/autophagy degradation pathway, and its degradation is delayed in GCD2 corneal fibroblasts. Further, the autophagy inducer rapamycin reduced the levels of cytosolic mutant TGF $\beta$ IP and attenuated its toxicity in GCD2 homozygous corneal fibroblasts. Furthermore, these data demonstrate that the aggregate-prone form of mutant TGF $\beta$ IP, unlike the WT protein, is strongly dependent on autophagy for clearance. In addition, we found that mutant TGF $\beta$ IP accumulates in lysosomes or autolysosomes in GCD2 corneal fibroblasts because of an impairment in autophagy (Choi et al., manuscript submitted). Therefore, these findings suggest that an autophagy inducer can also be used as a therapeutic drug for TGF $\beta$ -linked corneal dystrophies in the future.

The autophagy pathway is strongly regulated by levels of IP3, which acts as an endogenous autophagy inhibitor. In contrast, lithium promotes autophagy by blocking IP3 activity.<sup>38,44,45</sup> In this study, we found that lithium induces autophagy in corneal fibroblasts. Although we did not determine the levels of decreased TGF $\beta$ IP after the activation of autophagy with lithium, these findings suggest the therapeutic benefits of lithium in TGF $\beta$ -linked corneal dystrophies. In fact, given that lithium did not induce significant death in corneal fibroblasts even at very high concentrations (100 mM), it is highly likely that lithium can be used as a therapeutic agent for treating GCD2.

Studies have also demonstrated that the cytoprotective effects of lithium against oxidative stressors are dependent on the blockage of cytochrome *c* release and caspase-3 activation.<sup>46</sup> Previously, we showed that oxidative stress is involved in the pathogenesis of GCD2.<sup>46</sup> One possible relationship between GSK-3 $\beta$  activity and oxidative stress has been well described.<sup>47</sup> Oxidative stress may promote degeneration and ultimate cell death through DNA fragmentation, lipid peroxidation, and induction of mitochondrial proapoptotic pathways involving caspases and GSK-3 $\beta$ .<sup>48</sup> In addition, efforts to understand the molecular mechanisms underlying the resistance of cells to hydrogen peroxide-induced oxidative stress have shown that reduced GSK-3 $\beta$  activity may be essential to cell survival. In addition, the treatment of cells with lithium as a GSK-3 $\beta$  inhibitor resulted in increased resistance to hydrogen peroxide-induced oxidative stress.<sup>49</sup> Interestingly, evidence exists showing that GSK-3 $\beta$  inhibition specifically protects cells from intrinsic oxidative stress.<sup>50</sup> Thus, GSK-3 $\beta$  plays an important role in PI3K- and Akt-mediated cell survival pathways. Lithium is known to have antiapoptotic effects by reducing the expression of multiple apoptotic proteins, such as p53, Bax, and caspases,<sup>23,51</sup> and by increasing Bcl-2 levels.<sup>52</sup> Therefore, we also suggest that lithium treatment of TGF $\beta$ -linked corneal dystrophies may have multifunctional benefits. Ultimately, lithium treatment may be effective in regulating TGF- $\beta$  signaling, autophagy, and oxidative stress in numerous diseases.

## References

- Skonier J, Neubauer M, Madisen L, Bennett K, Plowman GD, Purchio AF. cDNA cloning and sequence analysis of beta Ig-h3, a novel gene induced in a human adenocarcinoma cell line after treatment with transforming growth factor-beta. *DNA Cell Biol.* 1992;11:511-522.
- Zhao Y, Shao G, Piao CQ, Berenguer J, Hei TK. Down-regulation of Betaig-h3 gene is involved in the tumorigenesis in human bronchial epithelial cells induced by heavy-ion radiation. *Radiat Res.* 2004;162:655-659.
- Zhao YL, Piao CQ, Hei TK. Downregulation of Betaig-h3 gene is causally linked to tumorigenic phenotype in asbestos treated immortalized human bronchial epithelial cells. *Oncogene.* 2002;21:7471-7477.
- Zhang Y, Wen G, Shao G, et al. TGFBI deficiency predisposes mice to spontaneous tumor development. *Cancer Res.* 2009;69:37-44.
- LeBaron RG, Bezverkov KI, Zimmer MP, Pavelec R, Skonier J, Purchio AF. Beta IG-H3, a novel secretory protein inducible by transforming growth factor-beta, is present in normal skin and promotes the adhesion and spreading of dermal fibroblasts in vitro. *J Invest Dermatol.* 1995;104:844-849.
- Billings PC, Herrick DJ, Kucich U, et al. Extracellular matrix and nuclear localization of beta ig-h3 in human bladder smooth muscle and fibroblast cells. *J Cell Biochem.* 2000;79:261-273.
- Kim JE, Jeong HW, Nam JO, et al. Identification of motifs in the fasciclin domains of the transforming growth factor-beta-induced matrix protein betaig-h3 that interact with the alphavbeta5 integrin. *J Biol Chem.* 2002;277:46159-46165.
- Klintworth GK. Advances in the molecular genetics of corneal dystrophies. *Am J Ophthalmol.* 1999;128:747-754.
- Korvatska E, Henry H, Mashima Y, et al. Amyloid and non-amyloid forms of 5q31-linked corneal dystrophy resulting from keratopithelin mutations at Arg-124 are associated with abnormal turnover of the protein. *J Biol Chem.* 2000;275:11465-11469.
- Moon JW, Kim SW, Kim TI, Cristol SM, Chung ES, Kim EK. Homozygous granular corneal dystrophy type II (Avellino corneal dystrophy): natural history and progression after treatment. *Cornea.* 2007;26:1095-1100.
- Woodgett JR. Judging a protein by more than its name: GSK-3. *Sci STKE.* 2001;2001:re12.
- Cadigan KM, Nusse R. Wnt signaling: a common theme in animal development. *Genes Dev.* 1997;11:3286-3305.
- Wodarz A, Nusse R. Mechanisms of Wnt signaling in development. *Annu Rev Cell Dev Biol.* 1998;14:59-88.
- Frame S, Cohen P. GSK3 takes centre stage more than 20 years after its discovery. *Biochem J.* 2001;359:1-16.
- Grimes CA, Jope RS. The multifaceted roles of glycogen synthase kinase 3beta in cellular signaling. *Prog Neurobiol.* 2001;65:391-426.
- Hedgepeth CM, Conrad LJ, Zhang J, Huang HC, Lee VM, Klein PS. Activation of the Wnt signaling pathway: a molecular mechanism for lithium action. *Dev Biol.* 1997;185:82-91.
- Phiel CJ, Klein PS. Molecular targets of lithium action. *Annu Rev Pharmacol Toxicol.* 2001;41:789-813.
- Stambolic V, Ruel L, Woodgett JR. Lithium inhibits glycogen synthase kinase-3 activity and mimics wingless signalling in intact cells. *Curr Biol.* 1996;6:1664-1668.
- Klein PS, Melton DA. A molecular mechanism for the effect of lithium on development. *Proc Natl Acad Sci U S A.* 1996;93:8455-8459.
- Fukumoto T, Morinobu S, Okamoto Y, Kagaya A, Yamawaki S. Chronic lithium treatment increases the expression of brain-derived neurotrophic factor in the rat brain. *Psychopharmacology (Berl).* 2001;158:100-106.
- Gould TD, Manji HK. The Wnt signaling pathway in bipolar disorder. *Neuroscientist.* 2002;8:497-511.
- Doble BW, Woodgett JR. GSK-3: tricks of the trade for a multi-tasking kinase. *J Cell Sci.* 2003;116:1175-1186.
- Chalecka-Franaszek E, Chuang DM. Lithium activates the serine/threonine kinase Akt-1 and suppresses glutamate-induced inhibition of Akt-1 activity in neurons. *Proc Natl Acad Sci U S A.* 1999;96:8745-8750.
- De Sarno P, Li X, Jope RS. Regulation of Akt and glycogen synthase kinase-3 beta phosphorylation by sodium valproate and lithium. *Neuropharmacology.* 2002;43:1158-1164.

1. Skonier J, Neubauer M, Madisen L, Bennett K, Plowman GD, Purchio AF. cDNA cloning and sequence analysis of beta Ig-h3, a

25. Zhang F, Phiel CJ, Spece L, Gurvich N, Klein PS. Inhibitory phosphorylation of glycogen synthase kinase-3 (GSK-3) in response to lithium: evidence for autoregulation of GSK-3. *J Biol Chem.* 2003;278:33067-33077.
26. Gould TD, Quiroz JA, Singh J, Zarate CA, Manji HK. Emerging experimental therapeutics for bipolar disorder: insights from the molecular and cellular actions of current mood stabilizers. *Mol Psychiatry.* 2004;9:734-755.
27. Jope RS. Anti-bipolar therapy: mechanism of action of lithium. *Mol Psychiatry.* 1999;4:117-128.
28. Kirshenboim N, Plotkin B, Shlomo SB, Kaidanovich-Beilin O, Eldar-Finkelman H. Lithium-mediated phosphorylation of glycogen synthase kinase-3 $\beta$  involves PI3 kinase-dependent activation of protein kinase C- $\alpha$ . *J Mol Neurosci.* 2004;24:237-245.
29. Liang MH, Chuang DM. Regulation and function of glycogen synthase kinase-3 isoforms in neuronal survival. *J Biol Chem.* 2007;282:3904-3917.
30. Liang MH, Chuang DM. Differential roles of glycogen synthase kinase-3 isoforms in the regulation of transcriptional activation. *J Biol Chem.* 2006;281:30479-30484.
31. Derynck R, Zhang YE. Smad-dependent and Smad-independent pathways in TGF- $\beta$  family signalling. *Nature.* 2003;425:577-584.
32. Shi Y, Massague J. Mechanisms of TGF- $\beta$  signaling from cell membrane to the nucleus. *Cell.* 2003;113:685-700.
33. Sanyal S, Kim SM, Ramaswami M. Retrograde regulation in the CNS; neuron-specific interpretations of TGF- $\beta$  signaling. *Neuron.* 2004;41:845-848.
34. Gomes FC, Sousa Vde O, Romao L. Emerging roles for TGF- $\beta$ 1 in nervous system development. *Int J Dev Neurosci.* 2005;23:413-424.
35. Choi SI, Kim TI, Kim KS, et al. Decreased catalase expression and increased susceptibility to oxidative stress in primary cultured corneal fibroblasts from patients with granular corneal dystrophy type II. *Am J Pathol.* 2009;175:248-261.
36. Jester JV, Huang J, Fisher S, et al. Myofibroblast differentiation of normal human keratocytes and hTERT, extended-life human corneal fibroblasts. *Invest Ophthalmol Vis Sci.* 2003;44:1850-1858.
37. Guo X, Ramirez A, Waddell DS, Li Z, Liu X, Wang XF. Axin and GSK3- control Smad3 protein stability and modulate TGF-signaling. *Genes Dev.* 2008;22:106-120.
38. Sarkar S, Floto RA, Berger Z, et al. Lithium induces autophagy by inhibiting inositol monophosphatase. *J Cell Biol.* 2005;170:1101-1111.
39. Koike M, Shibata M, Waguri S, et al. Participation of autophagy in storage of lysosomes in neurons from mouse models of neuronal ceroid-lipofuscinoses (Batten disease). *Am J Pathol.* 2005;167:1713-1728.
40. Klionsky DJ, Abeliovich H, Agostinis P, et al. Guidelines for the use and interpretation of assays for monitoring autophagy in higher eukaryotes. *Autophagy.* 2008;4:151-175.
41. Jope RS. Lithium and GSK-3: one inhibitor, two inhibitory actions, multiple outcomes. *Trends Pharmacol Sci.* 2003;24:441-443.
42. Ryves WJ, Harwood AJ. Lithium inhibits glycogen synthase kinase-3 by competition for magnesium. *Biochem Biophys Res Commun.* 2001;280:720-725.
43. Millet C, Yamashita M, Heller M, Yu LR, Veenstra TD, Zhang YE. A negative feedback control of transforming growth factor- $\beta$  signaling by glycogen synthase kinase 3-mediated Smad3 linker phosphorylation at Ser-204. *J Biol Chem.* 2009;284:19808-19816.
44. Sarkar S, Krishna G, Imarisio S, Saiki S, O'Kane CJ, Rubinsztein DC. A rational mechanism for combination treatment of Huntington's disease using lithium and rapamycin. *Hum Mol Genet.* 2008;17:170-178.
45. Sarkar S, Rubinsztein DC. Inositol and IP3 levels regulate autophagy: biology and therapeutic speculations. *Autophagy.* 2006;2:132-134.
46. Lai JS, Zhao C, Warsh JJ, Li PP. Cytoprotection by lithium and valproate varies between cell types and cellular stresses. *Eur J Pharmacol.* 2006;539:18-26.
47. Bowerman B. Cell biology: oxidative stress and cancer: a beta-catenin convergence. *Science.* 2005;308:1119-1120.
48. Maiese K, Chong ZZ. Insights into oxidative stress and potential novel therapeutic targets for Alzheimer disease. *Restor Neurol Neurosci.* 2004;22:87-104.
49. Schafer M, Goodenough S, Moosmann B, Behl C. Inhibition of glycogen synthase kinase 3  $\beta$  is involved in the resistance to oxidative stress in neuronal HT22 cells. *Brain Res.* 2004;1005:84-89.
50. King TD, Jope RS. Inhibition of glycogen synthase kinase-3 protects cells from intrinsic but not extrinsic oxidative stress. *Neuroreport.* 2005;16:597-601.
51. Chen RW, Chuang DM. Long term lithium treatment suppresses p53 and Bax expression but increases Bcl-2 expression: a prominent role in neuroprotection against excitotoxicity. *J Biol Chem.* 1999;274:6039-6042.
52. Rowe MK, Chuang DM. Lithium neuroprotection: molecular mechanisms and clinical implications. *Expert Rev Mol Med.* 2004;6:1-18.